Article

# Non-Base Pairing DNA Provides a New Dimension for Controlling Aptamer-Linked Nanoparticles and Sensors

Juewen Liu, and Yi Lu

*J. Am. Chem. Soc.*, **2007**, 129 (27), 8634-8643• DOI: 10.1021/ja072075+ • Publication Date (Web): 14 June 2007

J|A|C|S
ARTICLES
Published on Web 06/14/2007

# Non-Base Pairing DNA Provides a New Dimension for Controlling Aptamer-Linked Nanoparticles and Sensors

Juewen Liu and Yi Lu*

*Contribution from the Department of Chemistry and Beckman Institute for Advanced Science and Technology, University of Illinois at Urbana-Champaign, Urbana, Illinois 61801*

Received March 23, 2007; E-mail: yi-lu@uiuc.edu

***Abstract:*** DNA aptamers have been recently applied as simple and fast colorimetric sensors for a wide range of molecules. A unique feature of these systems is the presence of non-base pairing oligonucleotides in both DNA aptamers and spacers on DNA-functionalized nanoparticles. We report here a systematic investigation on an adenosine aptamer-linked gold nanoparticle system. When the aptamer overhang and the spacer were aligned on the same side, adenosine-responsive disassembly was inhibited. This inhibition effect increased with the length of the spacer, and fully inhibited activity was observed with the spacer containing more than three nucleotides. In contrast to a linear relationship between the spacer length and melting temperature in double-stranded DNA systems without overhangs, the aptamer system displayed a nonlinear relationship, with the melting temperature decreasing exponentially with spacer length. Control experiments suggested that this inhibition effect was due to thermodynamic factors rather than kinetic traps. A comparison with aptamer beacon systems indicated that nanoparticles may play an important role in this inhibition effect, and no specific interactions between the aptamer overhang and spacer were detected. The identity of nucleotides in the spacer did not affect the conclusions. Furthermore, the rate of disassembly or color change was slower at lower temperature or higher ionic strength, but was little affected by pH from 5.2 to 9.2. Therefore, non-base pairing DNA provided another dimension for controlling DNA-linked nanoparticles in addition to pH, temperature, or ionic strength, and this knowledge has resulted in the most optimal construct for sensing applications.

## Introduction

Because of its predictable secondary structure, ease of synthesis, and high stability, DNA has been widely used as templates for directed assembly or disassembly of nanomaterials.[1−9] For example, DNA has been designed to form sophisticated geometric structures, upon which nanoparticles or proteins were deposited to produce well-defined patterns.[10−15] DNA has also been used to template the synthesis of nanoparticle oligomers and polymers in a programmable manner.[16−19] An important direction in this field is DNA-templated assembly or disassembly of nanomaterials in response to chemical and biological stimuli, as such an endeavor has resulted in practical applications in colorimetric sensing of a diverse range of analytes, such as proteins,[20,21] DNA,[22−24] metal ions,[25−31] and small organic molecules.[32−36]

(1) Storhoff, J. J.; Mirkin, C. A. *Chem. Rev.* **1999**, *99*, 1849−1862.
(2) *WTEC Panel Report on Nanostructure Science and Technology: R&D Status and Trends in Nanoparticles, Nanostructured Materials, and Nanodevices*; Siegel, R. W., Hu, E., Roco, M. C., Eds.; Kluwer: Dordrecht, The Netherlands, 1999.
(3) Seeman, N. C. *Nature* **2003**, *421*, 427−431.
(4) Katz, E.; Willner, I. *Angew. Chem., Int. Ed.* **2004**, *43*, 6042−6108.
(5) Liu, J. W.; Lu, Y. *J. Fluoresc.* **2004**, *14*, 343−354.
(6) Feldkamp, U.; Niemeyer, C. M. *Angew. Chem., Int. Ed.* **2006**, *45*, 1856−1876.
(7) Lu, Y.; Liu, J. *Curr. Opin. Biotechnol.* **2006**, *17*, 580−588.
(8) Navani, N. K.; Li, Y. *Curr. Opin. Chem. Biol.* **2006**, *10*, 272−281.
(9) Lu, Y.; Liu, J. *Acc. Chem. Res.* **2007**, *40*, 315−323.
(10) Winfree, E.; Liu, F.; Wenzler, L. A.; Seeman, N. C. *Nature* **1998**, *394*, 539−544.
(11) Xiao, S.; Liu, F.; Rosen, A. E.; Hainfeld, J. F.; Seeman, N. C.; Musier-Forsyth, K.; Kiehl, R. A. *J. Nanopart. Res.* **2002**, *4*, 313−317.
(12) Yan, H.; Park, S. H.; Finkelstein, G.; Reif, J. H.; LaBean, T. H. *Science* **2003**, *301*, 1882−1884.
(13) Deng, Z.; Tian, Y.; Lee, S.-H.; Ribbe, A. E.; Mao, C. *Angew. Chem., Int. Ed.* **2005**, *44*, 3582−3585.
(14) Lin, C.; Katilius, E.; Liu, Y.; Zhang, J.; Yan, H. *Angew. Chem., Int. Ed.* **2006**, *45*, 5296−5301.
(15) Sharma, J.; Chhabra, R.; Liu, Y.; Ke, Y.; Yan, H. *Angew. Chem., Int. Ed.* **2006**, *45*, 730−735.
(16) Alivisatos, A. P.; Johnsson, K. P.; Peng, X.; Wilson, T. E.; Loweth, C. J.; Bruchez, M. P., Jr.; Schultz, P. G. *Nature* **1996**, *382*, 609−611.
(17) Mirkin, C. A.; Letsinger, R. L.; Mucic, R. C.; Storhoff, J. J. *Nature* **1996**, *382*, 607−609.
(18) Liu, Y.; Lin, C.; Li, H.; Yan, H. *Angew. Chem., Int. Ed.* **2005**, *44*, 4333−4338.
(19) Zhao, W.; Gao, Y.; Kandadai, S. A.; Brook, M. A.; Li, Y. *Angew. Chem., Int. Ed.* **2006**, *45*, 2409−2413.
(20) Pavlov, V.; Xiao, Y.; Shlyahovsky, B.; Willner, I. *J. Am. Chem. Soc.* **2004**, *126*, 11768−11769.
(21) Huang, C.-C.; Huang, Y.-F.; Cao, Z.; Tan, W.; Chang, H.-T. *Anal. Chem.* **2005**, *77*, 5735−5741.
(22) Elghanian, R.; Storhoff, J. J.; Mucic, R. C.; Letsinger, R. L.; Mirkin, C. A. *Science* **1997**, *277*, 1078−1080.
(23) Storhoff, J. J.; Elghanian, R.; Mucic, R. C.; Mirkin, C. A.; Letsinger, R. L. *J. Am. Chem. Soc.* **1998**, *120*, 1959−1964.
(24) Hazarika, P.; Ceyhan, B.; Niemeyer, C. M. *Angew. Chem., Int. Ed.* **2004**, *43*, 6469−6471.
(25) Liu, J.; Lu, Y. *J. Am. Chem. Soc.* **2003**, *125*, 6642−6643.
(26) Liu, J.; Lu, Y. *Chem. Mater.* **2004**, *16*, 3231−3238.
(27) Liu, J.; Lu, Y. *J. Am. Chem. Soc.* **2004**, *126*, 12298−12305.
(28) Liu, J.; Wernette, D. P.; Lu, Y. *Angew. Chem., Int. Ed.* **2005**, *44*, 7290−7293.
(29) Liu, J.; Lu, Y. *J. Am. Chem. Soc.* **2005**, *127*, 12677−12683.
(30) Liu, J.; Lu, Y. *Org. Biomol. Chem.* **2006**, *4*, 3435−3441.
(31) Wang, L.; Liu, X.; Hu, X.; Song, S.; Fan, C. *Chem. Commun.* **2006**, 3780−3782.
(32) Liu, J.; Lu, Y. *Anal. Chem.* **2004**, *76*, 1627−1632.


**10.1021/ja072075+ CCC: $37.00** 

To control disassembly of DNA-linked gold nanoparticles (AuNPs), a number of external stimuli have been employed. Mirkin and co-workers first demonstrated temperature-induced disassembly.[22,23,37] At temperatures higher than the melting temperature ($T_m$) of assembled AuNPs, NPs dispersed into solution because of thermal denaturation of DNA. In addition to thermal denaturation, disassemblies induced by biological and chemical stimuli have also been reported. For example, Niemeyer and co-workers prepared DNA-linked AuNPs in such a way that the linker DNA contained an overhang after pairing with the DNA on AuNPs.[24] By adding another DNA complementary to the linker DNA, AuNPs were disassembled because the linker DNA formed a more stable double helical structure with the added DNA.

In addition to solely relying on the base-pairing hybridization property of double-stranded DNA, a new class of DNA called functional DNA has also been used for directed assembly and disassembly of nanomaterials and colorimetric sensing.[5,7−9,25−36,38,39] Functional DNA is DNA with functions beyond genetic information storage and possesses properties similar to those of proteins, including catalysis (called DNAzymes, catalytic DNA, or deoxyribozymes), specific ligand binding (called aptamers),[40,41] or a combination of both (called aptazymes). They are obtained from a combinatorial biology process called in vitro selection or Systematic Evolution of Ligands by EXponential enrichment (SELEX). Since these functional DNA can recognize a wide range of molecules highly specifically, employing them for nanomaterial assembly can broaden the variety of stimuli to trigger the assembly process and the range of analytes for colorimetric sensing.[7,8] Therefore, we employed a $Pb^{2+}$-specific DNAzyme to assemble AuNPs. In the presence of $Pb^{2+}$, the substrate strand of the DNAzyme (served as a linker) was cleaved into two pieces, and AuNPs were disassembled.[28−30] Recently, we prepared aptamer-linked AuNPs.[33−36,39] In the presence of target analytes, AuNPs rapidly disassembled because the aptamers switched their structures and bound to target molecules instead of hybridizing to the DNA on AuNPs. The change of AuNP assembly state accompanied with a distinct color change and we have developed a general colorimetric sensing strategy.[35] For example, sensors for adenosine, cocaine, potassium ion, and their combinations were demonstrated.[34,35] In addition to its generality, this sensor design possesses the following advantages. First, compared to aptamer-based fluorescent sensors,[42−50] colorimetric sensors can eliminate the use of analytical instruments and make on-site detection easier.[20,21,31,33−35,51−53] Second, these sensors have fast responses and show instant color change upon addition of target molecules. Third, the detection can be carried out at room temperature with only a simple mixing step needed. Finally, AuNPs also have protection effects on DNA and DNA aptamers. These nanostructures can detect analytes in undiluted human blood serum,[36] and even after soaking in 10% serum for 17 h, the sensor color change can still be observed.[39] With separation technologies such as lateral flow devices to reduce background color,[36] the sensor sensitivity can rival fluorescence sensors.[43,47]

Because functional DNA molecules have been used for directed assembly of nanomaterials only recently, their interactions with nanomaterials are not well understood. Therefore, comprehensive investigations of such aptamer/nanoparticle systems will make important contributions to fundamental principles of biopolymer/nanomaterials interactions;[37,54−56] colorimetric sensor performance will also be improved with this knowledge. We report herein such an investigation. Differing from most previous studies, which focused on DNA base pairing interactions,[37,56,57] the current study focused on non-base pairing regions.[37,58] We found that non-base pairing regions of functional DNA played critical roles in stimuli-responsive assembly and disassembly and colorimetric sensing; by changing the relative position of aptamers and by inserting nucleotide spacers on AuNPs, the stability and activity of AuNP and aptamer systems changed drastically, even though all the thermodynamic conditions and base pairing interactions were kept constant. With such an understanding, we have an additional dimension of controlling the property of biopolymer-linked nanomaterials in addition to pH, ionic strength, or temperature, and the colorimetric sensors are much more robust after optimizations based on these findings.

## Results and Discussion

**Adenosine-Responsive Aptamer-Linked AuNP Disassembly System.** To investigate the interaction between aptamers and AuNPs, the adenosine aptamer-linked AuNPs were studied as a model system (Figure 1).[35] The system contained two kinds of DNA-functionalized AuNPs and a linker DNA ($Linker_{Ade}$). The linker DNA contained an adenosine aptamer fragment[59] (in green) and an extension (in gray and purple). The purple part of the linker hybridized to one kind of AuNP (functionalized with DNA shown in orange), while the gray part and a small fraction of the green part of the linker hybridized to the other kind of AuNP (functionalized with DNA shown in black). The aggregated AuNPs displayed a purple color in solution. In the presence of adenosine, the aptamer part bound adenosine and folded to the complex structure. As a result, only the gray part

(33) Liu, J.; Lu, Y. *Nat. Protoc.* **2006**, *1*, 246−252.
(34) Liu, J.; Lu, Y. *Adv. Mater.* **2006**, *18*, 1667−1671.
(35) Liu, J.; Lu, Y. *Angew. Chem., Int. Ed.* **2006**, *45*, 90−94.
(36) Liu, J.; Mazumdar, D.; Lu, Y. *Angew. Chem., Int. Ed.* **2006**, *45*, 7955−7959.
(37) Jin, R.; Wu, G.; Li, Z.; Mirkin, C. A.; Schatz, G. C. *J. Am. Chem. Soc.* **2003**, *125*, 1643−1654.
(38) Lu, Y. *Chem.−Eur. J.* **2002**, *8*, 4588−4596.
(39) Liu, J.; Lee, J. H.; Lu, Y. *Anal. Chem.* **2007**, *79*, 4120−4125.
(40) Tuerk, C.; Gold, L. *Science* **1990**, *249*, 505−510.
(41) Ellington, A. D.; Szostak, J. W. *Nature* **1990**, *346*, 818−822.
(42) Yamamoto, R.; Baba, T.; Kumar, P. K. *Genes Cells* **2000**, *5*, 389−396.
(43) Jhaveri, S. D.; Kirby, R.; Conrad, R.; Maglott, E. J.; Bowser, M.; Kennedy, R. T.; Glick, G.; Ellington, A. D. *J. Am. Chem. Soc.* **2000**, *122*, 2469−2473.
(44) Fang, X.; Cao, Z.; Beck, T.; Tan, W. *Anal. Chem.* **2001**, *73*, 5752−5757.
(45) Stojanovic, M. N.; de Prada, P.; Landry, D. W. *J. Am. Chem. Soc.* **2000**, *122*, 11547−11548.
(46) Stojanovic, M. N.; de Prada, P.; Landry, D. W. *J. Am. Chem. Soc.* **2001**, *123*, 4928−4931.
(47) Nutiu, R.; Li, Y. *J. Am. Chem. Soc.* **2003**, *125*, 4771−4778.
(48) Nutiu, R.; Li, Y. *Chem.−Eur. J.* **2004**, *10*, 1868−1876.
(49) Li, J. J.; Fang, X.; Tan, W. *Biochem. Biophys. Res. Commun.* **2002**, *292*, 31−40.
(50) Hamaguchi, N.; Ellington, A.; Stanton, M. *Anal. Biochem.* **2001**, *294*, 126−131.
(51) Stojanovic, M. N.; Landry, D. W. *J. Am. Chem. Soc.* **2002**, *124*, 9678−9679.
(52) Ho, H.-A.; Leclerc, M. *J. Am. Chem. Soc.* **2004**, *126*, 1384−1387.
(53) Famulok, M.; Mayer, G. *Nature* **2006**, *439*, 666−669.
(54) He, X.-X.; Wang, K.; Tan, W.; Liu, B.; Lin, X.; He, C.; Li, D.; Huang, S.; Li, J. *J. Am. Chem. Soc.* **2003**, *125*, 7168−7169.
(55) Vertegel, A. A.; Siegel, R. W.; Dordick, J. S. *Langmuir* **2004**, *20*, 6800−6807.
(56) Storhoff, J. J.; Lazarides, A. A.; Mucic, R. C.; Mirkin, C. A.; Letsinger, R. L.; Schatz, G. C. *J. Am. Chem. Soc.* **2000**, *122*, 4640−4650.
(57) Park, S. Y.; Lee, J.-S.; Georganopoulou, D.; Mirkin, C. A.; Schatz, G. C. *J Phys. Chem. B* **2006**, *110*, 12673−12681.
(58) Storhoff, J. J.; Elghanian, R.; Mirkin, C. A.; Letsinger, R. L. *Langmuir* **2002**, *18*, 6666−6670.
(59) Huizenga, D. E.; Szostak, J. W. *Biochemistry* **1995**, *34*, 656−665.

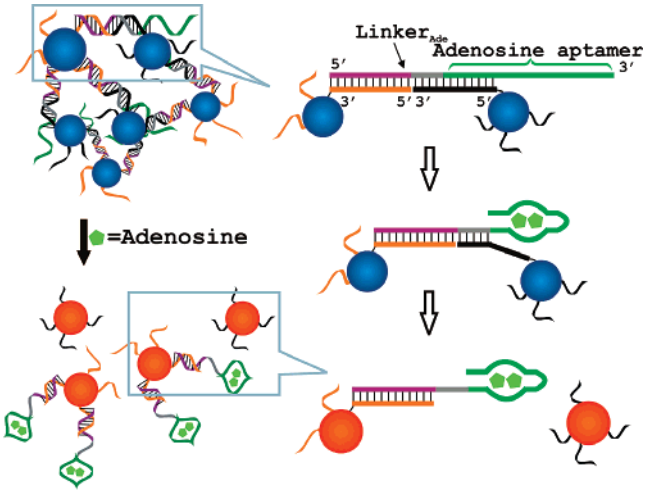


***Figure 1.*** Schematics of adenosine-induced disassembly of AuNPs linked by a DNA containing an adenosine aptamer. Each aptamer binds two adenosine molecules.

on the linker DNA was left to bind to the AuNP, which was unstable at room temperature, and the AuNP was released into solution, changing the solution color from purple to red. The design relies on the structure-switching properties of aptamers upon binding to their target molecules.[47,48,60−63] Because there are no special requirements on the aptamer part, the design is generally applicable to many aptamers.

The color change can be conveniently monitored by the naked eye or by UV−vis spectroscopy (Figure 2E). Upon addition of adenosine, the extinction at 522 nm increased while the extinction at 700 nm decreased. The extinction ratio at the two wavelengths was chosen to quantify the color of the system, with a high ratio associated with dispersed particles of red color and a low ratio associated with aggregated particles of purple color.[35] The color of the AuNPs in the presence of different nucleosides is shown in the inset of Figure 2E. Only the sample with adenosine displayed a red color, suggesting high analyte specificity.

For practical sensing applications, the aggregated AuNPs should be very stable in the absence of target analytes, while can still undergo fast disassembly and color change upon addition of targets. In addition to screening thermodynamic parameters such as temperature, pH, and ionic strength to search for optimal detection conditions, we aim to study the aptamer/AuNP system through varying its structure by introducing non-base pairing DNA spacers and changing AuNP size and alignment. At nanometer scale, where the sizes of nanoparticles and biopolymers are comparable, such structural changes may significantly affect the performance of the whole system. Our goal is to find the optimal condition under which the system has the highest stability and activity.

**Effects of Poly-Adenine Spacer and Aptamer Overhang on $T_m$.** Previous studies of double-stranded DNA-linked AuNPs (no overhangs on the linker DNA) showed that the $T_m$ was higher when AuNPs were functionalized with DNA containing a poly-adenine spacer inserted between the thiol group and the hybridization sequences.[37] Such an increase in $T_m$ was attributed to the increased distance between AuNPs.[37,58] Therefore, we first tested the effect of introducing a 12-mer adenine spacer ($A_{12}$) into the aptamer-linked AuNP system which, in contrast to the previously reported systems, contained an aptamer overhang with a number of non-base pairing nucleotides. As a result, the AuNP aggregates might have different properties depending on where the $A_{12}$ spacer was introduced. To investigate the spacer/overhang effect systematically, all four possible combinations were tested as shown in Figure 2A−D. There were two kinds of AuNPs in each case, functionalized with 3′- and 5′-thiol-modified DNA, respectively. Although each aggregate contained thousands of AuNPs, for clarity reasons, only two were drawn in the figure to show the connection. None of the two AuNPs in Figure 2A ($A_0$1, $A_0$2) contained the $A_{12}$ spacer, and this aggregate had the lowest melting temperature ($T_m$ = 30 °C, Figure 2F, black curve). When both AuNPs contained the spacer ($A_{12}$1, $A_{12}$2 in Figure 2D), the $T_m$ was the highest ($T_m$ = 47 °C, Figure 2F, green curve), which was consistent with literature reports that inserting poly-A spacers increased $T_m$.[37] Interestingly, the other two samples with only one AuNP containing the $A_{12}$ spacer also showed very different $T_m$ values. Placing the spacer away from the aptamer overhang (Figure 2B) increased $T_m$ by 5 °C ($T_m$ = 35 °C, Figure 2F, blue curve) compared to the construct shown in Figure 2A; adding the spacer to the same side (Figure 2C) increased $T_m$ by 13 °C ($T_m$ = 43 ° C, Figure 2F, red curve). This difference was attributed to the aptamer overhang in the linker DNA posing additional steric effects to make the system more crowded. Introducing a spacer on the same side with the aptamer overhang (Figure 2C) not only increased AuNP spacing but also relieved steric effects resulted from the aptamer overhang, allowing a higher increase in $T_m$. In some melting curves, extinction decrease with increase of temperature was observed before the melting transition (i.e., the green curve in Figure 2F). This phenomenon has been characterized in detail by Mirkin and co-workers and is known as the annealing effect in which AuNPs are packing into more stable structures with the energy provided by increased temperature.[56]

**Effects of Poly-Adenine Spacer and Temperature on Activity.** To identify the optimal construct for sensing applications, the kinetics of color change of the four nanostructures shown in Figure 2A−D in the absence or presence of 1 mM adenosine was monitored at various temperatures (Figure 3). For the system in Figure 2A, since $T_m$ was determined to be 30 °C and the extinction at 260 nm started to increase at ∼23 °C (Figure 2F, black curve), kinetics of adenosine-induced disassembly was monitored at 10, 15, and 20 °C (Figure 3A−C) to avoid background disassembly induced by temperature. In each figure, the blue and red curves correspond to the kinetic traces in the absence and presence of 1 mM adenosine, respectively. The blue curves were flat in all the systems, indicating the absence of background color change induced by temperature. Adenosine-induced color changes were observed at all three temperatures, with the fastest rate being at 20 °C. For the system in Figure 2B, disassembly kinetics at 16, 21, and 26 °C was monitored (Figure 3D−F) for the same reason discussed above. A similar trend was observed with the rate being the fastest at the highest temperature tested. Surprisingly, no disassembly or

(60) Nutiu, R.; Mei, S.; Liu, Z.; Li, Y. *Pure Appl. Chem.* **2004**, *76*, 1547−1561.
(61) Hartig, J. S.; Najafi-Shoushtari, S. H.; Gruene, I.; Yan, A.; Ellington, A. D.; Famulok, M. *Nat. Biotechnol.* **2002**, *20*, 717−722.
(62) Rupcich, N.; Nutiu, R.; Li, Y.; Brennan, J. D. *Angew. Chem., Int. Ed.* **2006**, *45*, 3295−3299.
(63) Rupcich, N.; Nutiu, R.; Li, Y.; Brennan, J. D. *Anal. Chem.* **2005**, *77*, 4300−4307.

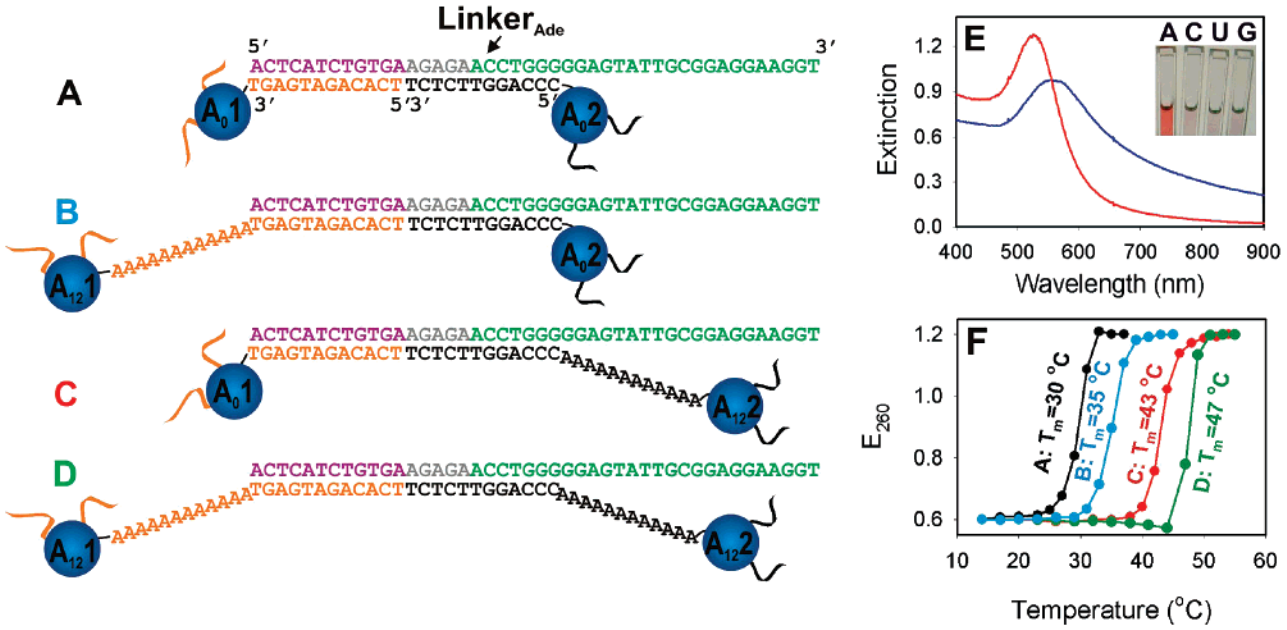


***Figure 2.*** (A−D). Four combinations of aptamer DNA-assembled AuNPs with or without an $A_{12}$ spacer. (E) Extinction spectra of AuNPs shown in Figure 2B before (blue) and 10 s after (red) adding 2 mM adenosine. (Inset) Photo of aptamer-linked AuNPs in the presence of 2 mM adenosine, cytosine, uridine, or guanosine (from left to right). (F) Melting curves of the four systems. $T_m$ of each curve is marked.

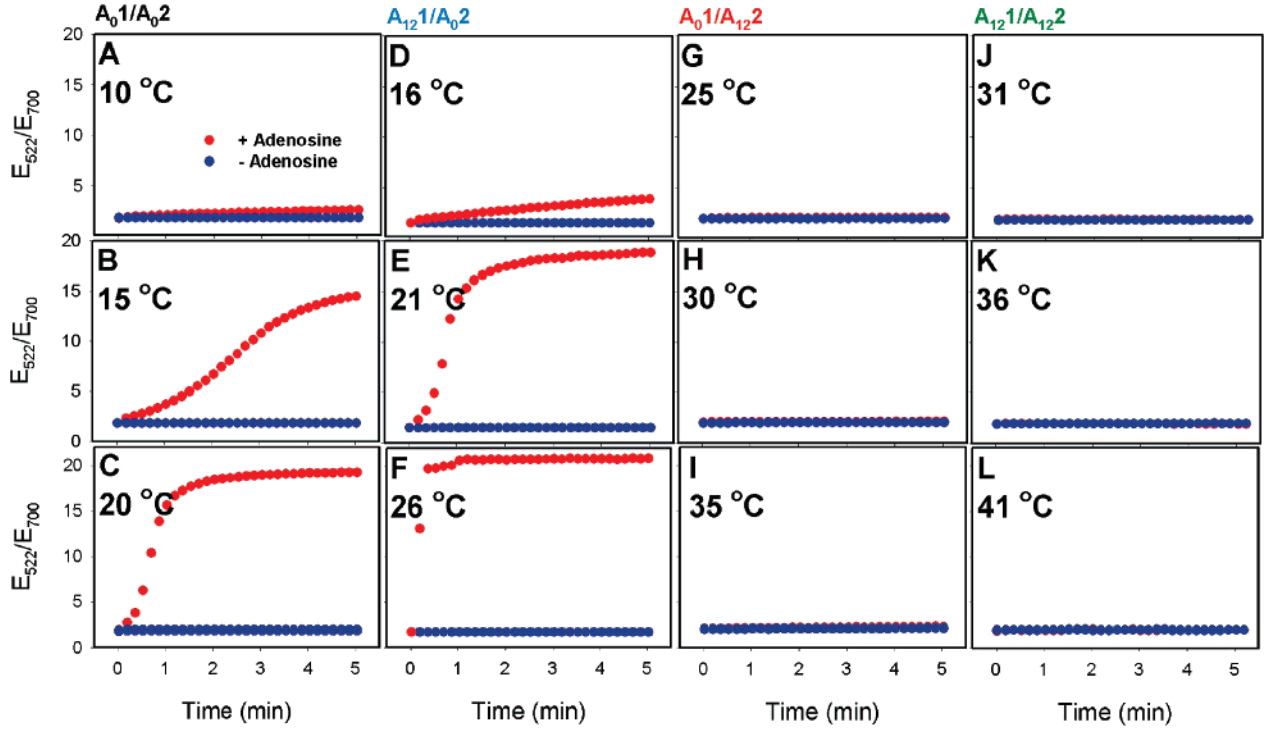


***Figure 3.*** Kinetics of adenosine-induced color change of AuNP aggregates at different temperatures. All four systems in Figure 2A−D were tested. (A−C) For Figure 2A, (D−F) Figure 2B, (G−I) Figure 2C, and (J−L) Figure 2D. Each figure contains two curves: Without (blue) or with (red) 1 mM adenosine. The highest temperature tested for each system was just below the temperature at which the AuNP aggregate started to melt.

color change was observed at all tested temperatures (Figure 3G−L) for the other two systems (Figure 2C,D). A common feature of these two constructs is that the aptamer overhang and the $A_{12}$ spacer were on the same side. The aptamer overhang could interact with the spacer and AuNP surface to inhibit aptamer-binding activities. Since this feature is unique for aptamer-linked nanostructures, it deserves further systematic investigations of the nature of such interactions, including the length and composition of the spacer. We previously reported adenosine concentration-dependent responses of aptamer-linked AuNPs for the construct shown in Figure 2B.[35] Higher levels of adenosine gave faster rates of color change. We chose 1 mM adenosine in the current study because it is in the saturation region (the $K_d$ value for this aptamer is 10 $\mu$M).[35,59]

**Effects of the Poly-Adenine Spacer Length.** Because an $A_{12}$ spacer on the same side of the aptamer inhibited color change, we wonder what is the minimum spacer length for the inhibition. To answer this question, six AuNP aggregates were

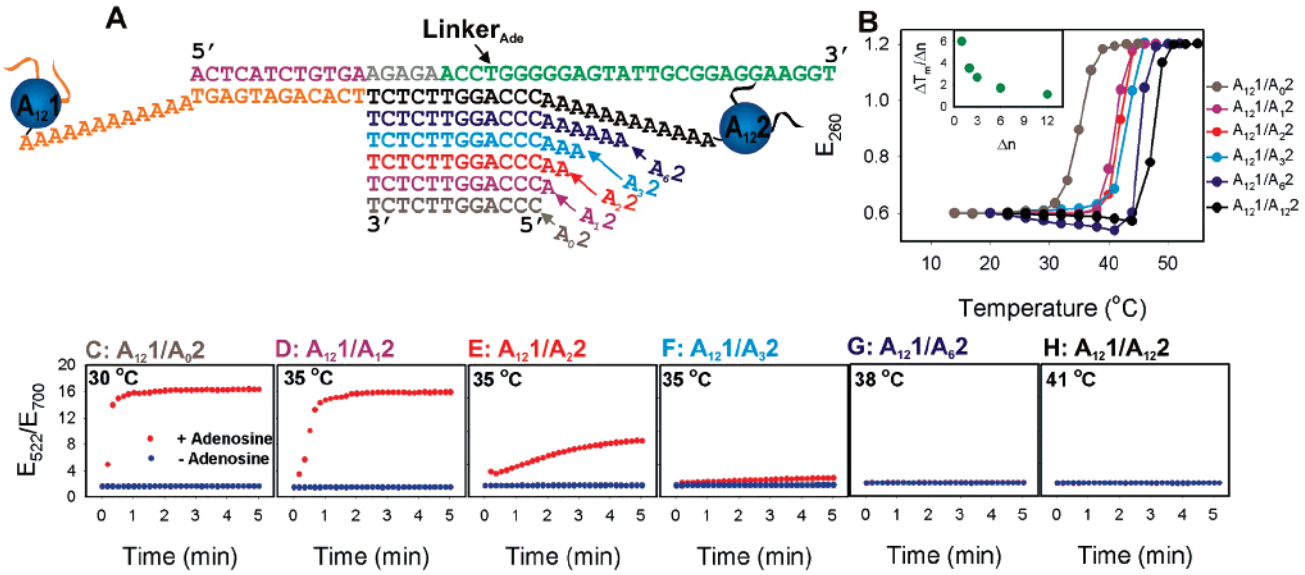


***Figure 4.*** (A) Six aptamer-linked AuNP systems with varying number of adenine in the spacer region. (B) Melting curves of the six systems. (Inset) Contribution to the increase of $T_m$ by each adenine as a function of the number of adenine in the spacer. (C−H) Kinetics of disassembly in the presence (red) or absence (blue) of 1 mM adenosine at designated temperatures for the six systems.

prepared (Figure 4A). These systems contained the same $A_{12}1$ AuNP (the NP on the left part of Figure 4A), while the number of adenines in the spacer of the 5′-thiol-modified DNA varied from 0 to 12 (NPs on the right). The melting curves of these six systems are shown in Figure 4B. It can be observed that $T_m$ increased with increasing spacer length. In a system where the linker DNA did not contain any overhang, Mirkin and co-workers reported that there was a linear relationship between the number of adenines in the spacer and $T_m$.[37] That means the increase of $T_m$ can be predicted by multiplying the number of adenines with a constant. In the current aptamer-linked system, however, the increase of $T_m$ as a function of the adenine spacer length was nonlinear. As can be observed from the inset of Figure 4B, the longer the spacer ($\Delta n$ on the *x*-axis), the smaller contribution to $T_m$ each adenine made ($\Delta T_m/\Delta n$ on the *y*-axis). The first adenine increased $T_m$ by 6 °C; inserting the second adenine resulted in an increase of only 3.5 °C by each one. Further increase of the spacer length decreased the contribution of each adenine even more. In addition to the nonlinear relationship, the increase on $T_m$ was much larger in the aptamer system (with an overhang) than that without an overhang. When no overhangs were present, the increase of $T_m$ by each adenine was calculated to be 0.327 °C (buffer contained 300 mM NaCl);[37] in the current aptamer system, the contribution of each adenine ranged from 1.1 to 6 °C (buffer contained 150 mM NaCl). In AuNP aggregates without a linker overhang, the $T_m$ increase was mainly from the increased particle-to-particle distance.[37] When an overhang was present, the spacer also relieved the steric effect of the overhang. Because of the twofold contributions, the $T_m$ increase in the aptamer system was nonlinear and larger in value.

At a temperature below but close to the $T_m$ of each system, the disassembly kinetics in the presence or absence of adenosine was compared. The sample without an adenine spacer ($A_0$) disassembled the fastest (Figure 4C). The samples with $A_1$, $A_2$, and $A_3$ spacers disassembled progressively slower (Figure 4D−F). Further increase of the spacer length completely inhibited the disassembly (Figure 4G,H). From the experiment, it can be concluded that the inhibition effect is proportional to the length of the spacer. Even though the overhang contained 20 nucleotides, an $A_3$ spacer can almost completely inhibit the disassembly, which demonstrated that the nature of the interaction between the overhang and the spacer was non-Watson−Crick base pairing interactions, as at least five adenines were need to interact with the first thymine in the overhang to form a base pair. The next question then is whether the effect is specific to poly-A spacers, or whether any nucleotide spacer has the same effect.

**Effects of the Spacer Composition.** To test the sequence specificity of spacer-inhibited disassembly, two additional constructs were prepared. One contained a $C_{12}$ spacer on the same side as the aptamer overhang (Figure 5C), and the other contained a $N_{12}$ spacer, which was a repeat of the CAGT sequences (Figure 5D). $G_{12}$ spacer was not tested because of synthetic difficulties; $T_{12}$ was not tested to avoid interactions with $A_{12}$ on AuNPs. AuNPs without any spacer (Figure 5A) and with an $A_{12}$ spacer (Figure 5B) were also prepared as positive and negative controls, respectively. Interestingly, the $C_{12}$ system (Figure 5C) had the highest $T_m$ (Figure 5E, blue curve), possibly due to formation of additional base pairs between the poly-C spacer and guanine bases in the aptamer overhang. The system with the $N_{12}$ spacer (Figure 5D) showed melting properties similar to that with $A_{12}$ (Figure 5B). However, neither $C_{12}$ nor $N_{12}$ systems showed adenosine-induced disassembly (Figure 5H,I), and disassembly was observed only in the absence of any spacer close to the aptamer overhang (Figure 5F).

**Effect of the Poly-A Spacer in Dispersed Aptamer Beacons.** Next, to find out whether the observed inhibition effect was unique to the AuNP system, a fluorescence resonance energy transfer (FRET)-based study without AuNPs was carried out. Two aptamer beacons were constructed as shown in Figure 6A,B. The same aptamer linker that had been used to assemble AuNPs was employed here to assemble fluorophore and quencher-labeled DNA. The two beacons had the same quencher-labeled DNA. For the fluorophore-labeled DNA, the one in

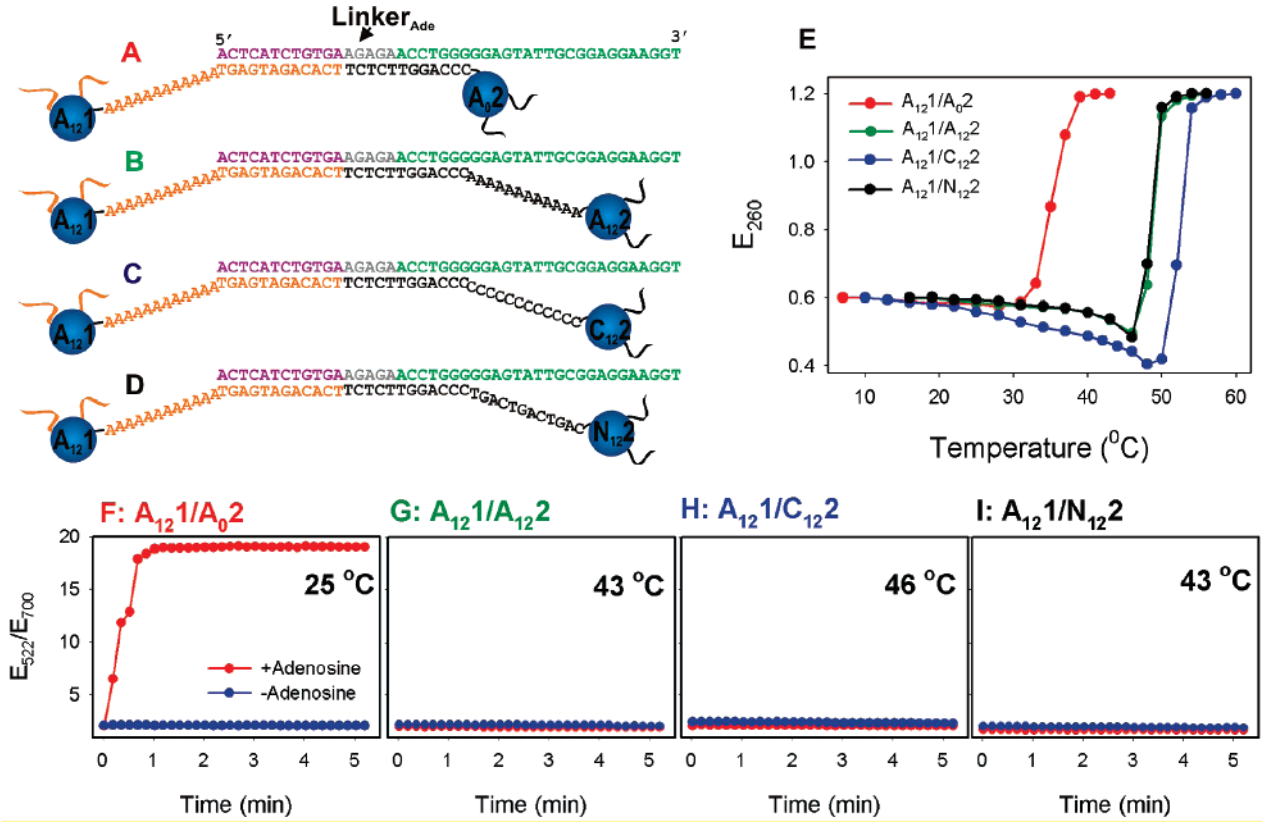


***Figure 5.*** (A−D) Four aptamer-linked AuNP aggregates with the 5′-thiol-functionalized DNA containing different nucleotide spacers. (E) Melting curves of the four systems. (F−I) Kinetics of disassembly of the four systems (A−D) in the presence (red) or absence (blue) of 1 mM adenosine.

Figure 6A did not contain any poly-A overhang, while the one in Figure 6B contained an $A_{12}$ overhang. Both DNAs had the same sequence as the thiol-modified DNA shown in Figure 2, except that the thiol modifications were eliminated. In the initial state, the fluorescence was quenched because of the proximity between the fluorophore and the quencher. Addition of adenosine could induce release of the fluorophore-labeled DNA and thus enhance fluorescence.[47] First, the melting curves of the two aptamer beacons were collected. Interestingly, the beacon containing an $A_{12}$ overhang (Figure 6B) showed slightly lower $T_m$ than that without the overhang (Figure 6C), which was the opposite of what was observed in the AuNP systems (Figure 2). The kinetics of fluorescence change in the presence or absence of adenosine was also recorded, and both beacons showed significant fluorescence increase (∼10-fold) with adenosine (Figure 6D,E). Therefore, the inhibited disassembly in AuNP systems was unique and not due to specific interactions (i.e., base pairing) between the aptamer overhang and the poly-A spacer; instead, AuNPs played an important role in such effects.

**General Applicability of the Observed Spacer and Overhang Effects.** To confirm the generality of the observed spacer and overhang effects, control experiments were designed by shuffling the aptamer fragment from the 3′-end to the 5′-end of the linker DNA (Figure 7A−D), and the new linker DNA was then named 5′Linker$_{Ade}$. Similarly, AuNPs were functionalized by DNA with or without an $A_{12}$ spacer, and four aptamer-linked systems were prepared. The melting temperatures were all different (Figure 7E), with the highest one containing the $A_{12}$ spacer in both particles (Figure 7D) and the lowest one containing no spacer (Figure 7A). For the remaining two systems with only one $A_{12}$ spacer, the higher $T_m$ went to the one with the spacer on the same side with the aptamer overhang (Figure 7B). The kinetics of adenosine-induced disassembly was also recorded for these aggregates, and color change was observed only when the aptamer overhang was on the opposite side of the $A_{12}$ spacer (Figure 7H for 7C) or in the absence of any spacer (Figure 7F for 7A). This experiment confirmed that the spacer and overhang effect was general for the adenosine aptamer system, no matter the position of the aptamer overhang.

To further confirm whether this effect can be generalized to other aptamer and nanoparticle systems, cocaine aptamer-linked AuNPs were also tested, and the results are presented in the Supporting Information. Similarly, incorporation of an $A_{12}$ spacer to the same side with the cocaine aptamer overhang inhibited disassembly. Therefore, the observed interactions between the aptamer overhang and the DNA spacer on AuNPs should be a general phenomenon. Understanding such interactions is important for improving sensor and materials design. The next question we want to address is the origin of the effect: Whether it is thermodynamic or kinetic.

**Investigation of the Origin of the Inhibition Effect.** There could be two reasons for the inhibited disassembly when the aptamer overhang aligned on the same side with the spacer. First, it could be that such arrangements were intrinsically thermodynamically more stable, and the aptamer tended to be in such a form rather than binding to its target. Second, it could be that the aptamer overhang was kinetically trapped by the spacer in the assembled state and thus inhibited its binding activity. To identify the cause, instead of performing adenosine-induced disassembly as shown in Figure 1, the reverse process or formation of aggregates from dispersed AuNPs in the presence or absence of adenosine was tested (Figure 8A). To

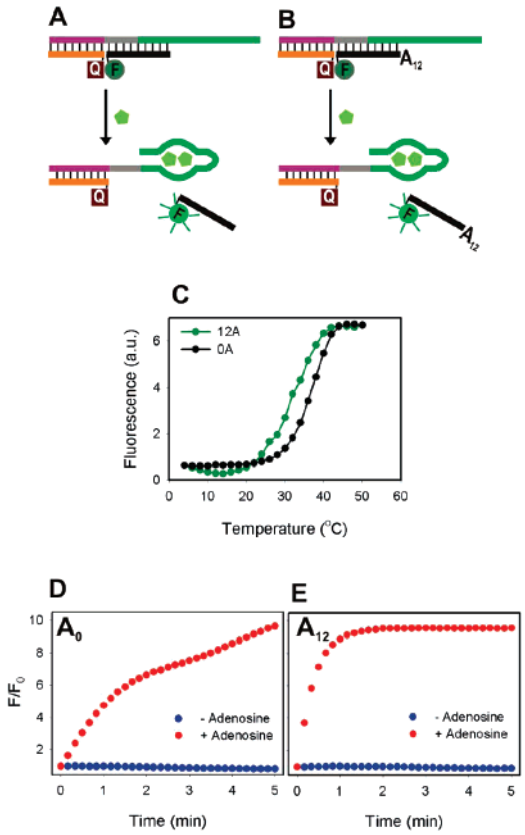


***Figure 6.*** Construction of aptamer beacons without (A) and with (B) an $A_{12}$ overhang on the same side with the aptamer overhang (green). Q and F denote quencher and fluorophore, respectively. (C) Fluorescence-based melting curves of the two aptamer beacons in 150 mM NaCl, 25 mM Tris acetate, pH 8.2 (the same buffer condition as the AuNP work). (D and E) Kinetics of fluorescence change for the aptamer beacons in (A) and (B), respectively, with or without 1 mM adenosine. The temperature was 10 °C for both reactions. The DNA sequences are in Supporting Information.

maximize the effect of adenosine, the NaCl concentration was systematically varied to search for the optimal thermodynamic condition, at which the NaCl concentration was just high enough to assemble AuNPs in the absence of adenosine. All the samples were incubated at 4 °C for AuNPs to assemble. As shown in Figure 8B (red bars for no adenosine), the extinction ratio decreased with increasing NaCl concentrations, suggesting formation of more aggregated AuNPs. In the presence of adenosine (black bars), however, the extinction ratios were only slightly higher in all the conditions. The differences in extinction ratios between fully assembled and fully disassembled AuNPs were usually larger than 15; the largest difference here was less than 3, and hardly any color difference can be observed by the naked eye. Because there should be no kinetic trap initially when all components were separated from each other, it was likely that when the overhang and the spacer were aligned on the same side, formation of AuNP aggregates was thermodynamically more favorable. Therefore, the failure to disassemble certain AuNP aggregates was mainly attributed to thermodynamic effects rather than kinetic traps; the aptamer was more stable with the spacer on the AuNP surface.

**Effects of Nanoparticle Alignment and Size.** In double-stranded DNA- or DNAzyme-linked AuNP systems, it has been shown that AuNP alignment has significant effects on their properties.[26,27,29,37] For example, in the $Pb^{2+}$-specific DNAzyme/AuNP system, the DNAzyme was active when AuNPs were aligned in a tail-to-tail manner, but not head-to-tail.[29] Therefore, the effect of AuNP alignment was also investigated in the aptamer system. In all the experiments presented thus far in this work, AuNPs were aligned in a tail-to-tail manner, in which the distance between the two AuNPs was long. By changing the position of the thiol groups, head-to-tail aligned AuNPs were prepared (Figure 9A,B). Compared to tail-to-tail aligned systems, head-to-tail aligned ones had lower $T_m$. For example, the $T_m$ for the system shown in Figure 9A was 22 °C (Figure 9E, black curve), while its tail-to-tail counterpart had a $T_m$ of 35 °C (Figure 2F, blue curve). Similarly, the system shown in Figure 9B had a $T_m$ of 42 °C (Figure 9E, blue curve), while its tail-to-tail counterpart had a $T_m$ of 47 °C (Figure 2F, green curve). Such differences in $T_m$ can be explained by the spacing between AuNPs.[37] Interestingly, both head-to-tail aligned systems showed adenosine-induced disassembly (Figure 9F,G). Therefore, even though head-to-tail aligned nanoparticles inhibited the activity of bridging DNAzymes,[29] the binding properties of aptamers were not affected.

For the head-to-tail aligned system in Figure 9B, even though both $A_{12}$ spacers were present, neither was close to the aptamer overhang because of the alignment of AuNPs. As a result, the effect of such a spacer was decreased. This suggested that, for the inhibition effect to take place, aptamer overhangs need to be spatially aligned close to the spacer on AuNP surface. It is worth pointing out that it was much more difficult for head-to-tail aligned AuNPs to form. Even after being incubated at 4 °C for 2 days, only ~50% of AuNPs were in the aggregated state; it took only several hours for tail-to-tail aligned AuNPs to aggregate completely.

The effect of AuNP size on the aptamer system was also studied. All the above data were collected with 13-nm diameter nanoparticles. Larger AuNPs of 40-nm diameter were assembled as shown in Figure 9C,D. Similar to 13-nm particles, the 40-nm particle assembled aggregates also showed higher $T_m$ with an $A_{12}$ spacer on the same side of the aptamer overhang (Figure 9H, green curve), which also showed inhibited disassembly (Figure 9J). The other configuration (Figure 9C) showed lower $T_m$ (Figure 9H, red curve) and fast color change (Figure 9I). Therefore, the size of AuNPs does not have significant effect on disassembly in the aptamer system.

**Effects of pH and Ionic Strength.** To reach a full understanding on the aptamer-linked AuNPs for sensing applications, the effects of pH and ionic strength were further investigated. The experiments were performed with the system shown in Figure 2B. At very low (pH < 4.2) or very high pH (pH > 10.2), AuNP aggregates were not stable and disassembled very quickly even in the absence of adenosine. This could be attributed to the denaturation of DNA at extreme pH conditions. For the pH range between the two extremes (pH 5.2−9.2), the rates of disassembly were very similar (Figure 10A−C), suggesting that binding of the aptamer fragment to adenosine can occur over a wide pH range. With increase of NaCl, the level of disassembly or color change decreased (Figure 10D−F). This trend was consistent with the temperature-dependent studies shown in Figure 3, where lower temperatures gave slower rates of disassembly. DNA duplexes were stabilized at high NaCl or low temperature, while the binding interaction between the aptamer and adenosine changed relatively less by these factors. As a result, it was relatively more difficult for an

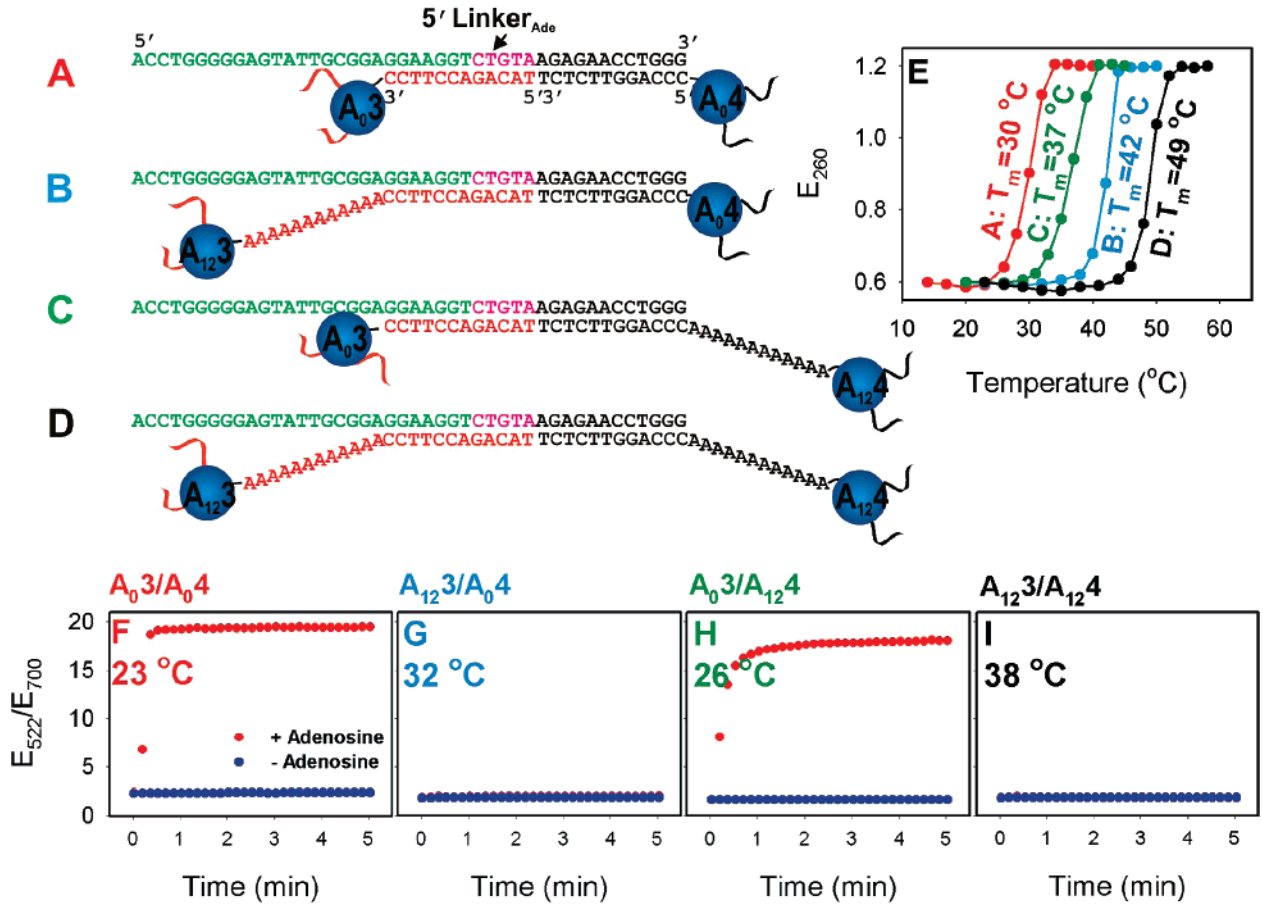


***Figure 7.*** (A−D) Four combinations of aptamer-linked AuNPs with or without a poly-A spacer in which the aptamer part (green) is at the 5′ region of the linker (5′Linker$_{Ade}$). (E) Melting curves of the four systems. $T_m$ of each curve is marked. (F−I) Kinetics of adenosine-induced color change for the four systems at temperature close to their $T_m$.

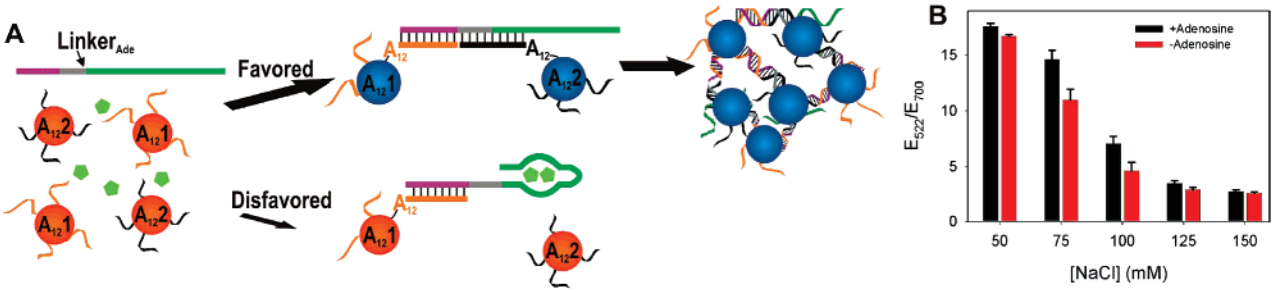


***Figure 8.*** (A) Schematic presentation of formation of AuNP aggregates in the presence of adenosine (green pentagons). With an $A_{12}$ spacer on the same side of the aptamer overhang, aggregate formation is favored even in the presence of adenosine. (B) Assembly state or color of the assembly system in the presence of varying concentrations of NaCl with (black bars) or without (red bars) 1 mM adenosine.

aptamer to compete with DNA base pairing interactions at higher ionic strength or lower temperature.

**Implications for Materials Design and Sensing Applications.** The aptamer-assembled AuNPs are capable of undergoing fast color change in the presence of target molecules, and therefore these materials are useful as colorimetric sensors.[33−36] To optimize sensor performance, thermodynamic factors are usually tuned, such as pH, ionic strength, and temperature. Results presented here indicate that non-base pairing regions of aptamer-linked nanostructures are a very important factor to consider. Systematic investigation and careful tuning of this factor can enhance sensor performance. For the four systems shown in Figure 2, two of them (Figure 2C,D) were incapable of changing color. For the other two (Figure 2A,B), the one in Figure 2B was superior, because under the same thermodynamic conditions, the Figure 2B system had higher stability and could still undergo fast adenosine-induced color change, which in turn allowed a wider window to accommodate thermodynamic variables. This study also demonstrates one of the advantages associated with the disassembly based sensor system. It may take a relatively long time for AuNP assembly to happen, and disassembly can take place instantaneously, which is important for sensing applications.

In the current system, there are more than 100 thiol-modified DNA on each 13-nm AuNP.[64] An interesting question to ask is whether the same spacer-induced inhibition effect can be observed on monofunctionalized AuNPs. In that case, AuNPs are no longer in cross-linked or aggregated form, but rather act

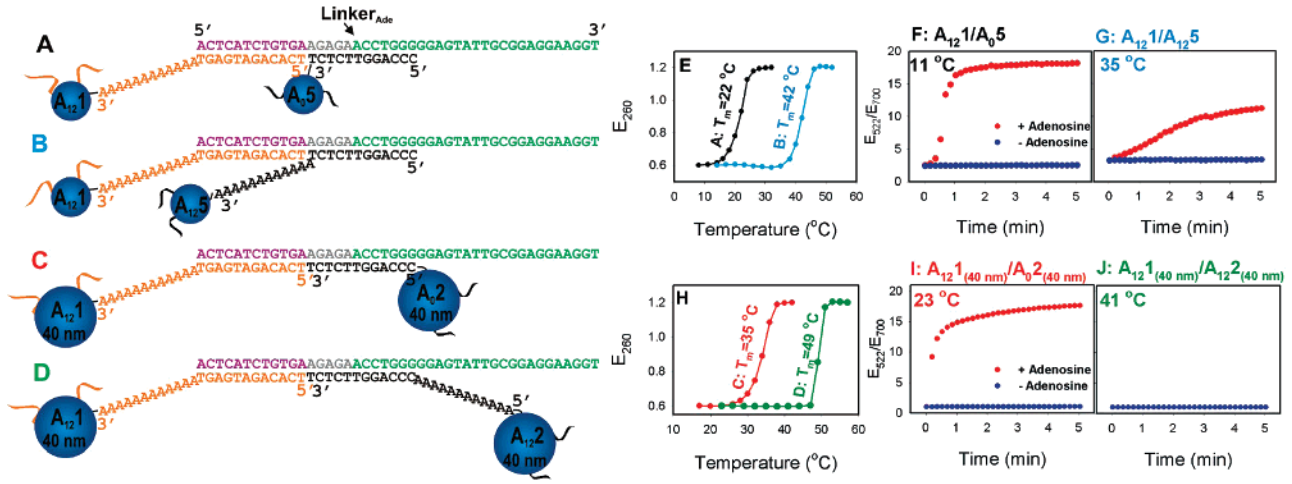


***Figure 9.*** Head-to-tail aligned AuNPs without (A) or with (B) an $A_{12}$ spacer close to the adenosine aptamer overhang. Tail-to-tail aligned AuNPs with 40 nm diameter nanoparticles without (C) or with (D) an $A_{12}$ spacer close to the adenosine aptamer. (E) Melting curves of the aggregates shown in (A) and (B). (F and G) Kinetics of disassembly in the presence (red) or absence (blue) of 1 mM adenosine for the aggregates in (A) and (B), respectively. (H) Melting curve of aggregates shown in (C) and (D). (I and J) Kinetics of disassembly in the presence or absence of 1 mM adenosine for aggregates in (C) and (D), respectively.

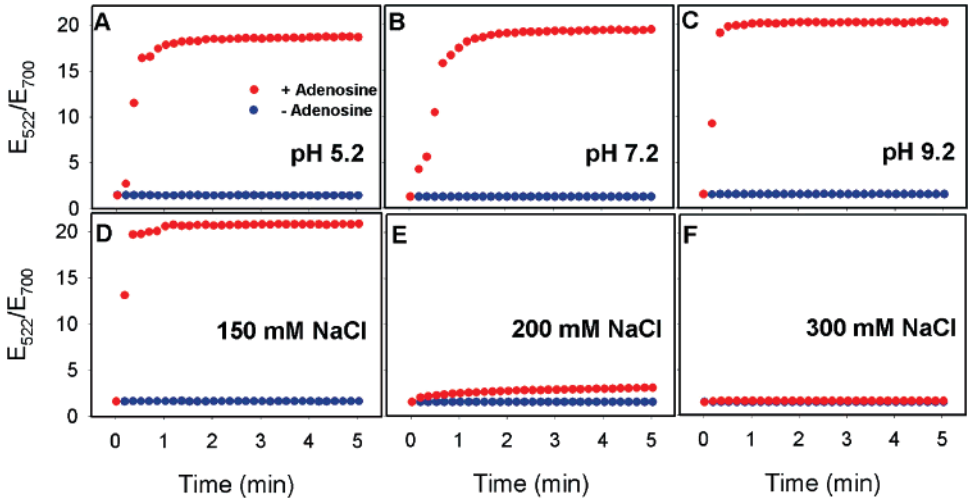


***Figure 10.*** (A−C) pH-dependent studies on the aptamer/AuNP system in Figure 2B. NaCl concentration was 150 mM, and temperature was 26 °C. (D−F) NaCl-dependent studies on the same system. pH was 8.2, and temperature was 26 °C. Adenosine concentration was either 0 or 1 mM for all the experiments.

as chromophore labels similar to those shown in Figure 6. Such an experiment may provide further insights on the nature of DNA/AuNP interactions and will be a subject of future studies. In this study, interactions between DNA and AuNPs were studied in detail, which was made possible by the large volume of work in the literature on this topic that provided experimental protocols and basis for comparison.[17,22,23,37,56−58] In addition to serving as a model system to understand nanoparticles/biopolymer interactions, AuNPs are also technically important and their applications in sensing, diagnostics, nanotechnology, and materials science and engineering have been witnessed in the past decade.[1−9] Detailed studies on interactions between other nanomaterials and DNA (or even other biopolymers) are expected with the development of the chemistry and characterization tools in those systems.

This aptamer-linked AuNP system is also proven to be a useful platform for systematic study of nanoparticle/biopolymer interactions. On the one hand, nucleic acid sequences and nanoparticle alignment, size, or composition can be conveniently varied; on the other hand, the effect of changing these parameters can be conveniently monitored through distinct color changes. Given the significant progress made on using nanoparticles for varying applications,[1−9,65] continuation on the characterization of biopolymer/nanomaterials interactions is likely to grow. Having such systems that possess activity, tunable properties, and easy readouts can help to design better biomaterials.

## Conclusions

In summary, adenosine-induced disassembly of aptamer-linked AuNPs was studied in detail. Such aptamer-linked AuNPs are useful colorimetric sensors for a broad range of analytes. Unlike most previously reported systems, an aptamer overhang was present here. It was demonstrated that the alignment between the aptamer overhang and oligonucleotide spacers on AuNPs had a significant influence on the kinetics of disassembly. Such effects can be fine-tuned, and even a single nucleotide change in the spacer region can have a large effect.

(64) Demers, L. M.; Mirkin, C. A.; Mucic, R. C.; Reynolds, R. A., III; Letsinger, R. L.; Elghanian, R.; Viswanadham, G. *Anal. Chem.* **2000**, *72*, 5535−5541.

(65) Rosi, N. L.; Mirkin, C. A. *Chem. Rev.* **2005**, *105*, 1547−1562.

Importantly, the effect was observed only in aggregated nanoparticles but not in dispersed aptamer beacons, suggesting the presence of special aptamer/AuNP interactions mediated by nucleic acid spacers. Experiments also showed that the origin of the effect was thermodynamic instead of kinetic. The effects of other factors on the disassembly kinetics, such as AuNP size and alignment, temperature, ionic strength, and pH, were also studied to fully characterize the system. Among the three classes of DNA molecules mentioned in this article, double-stranded DNA, DNAzymes, and DNA aptamers, DNA aptamers recognize the broadest range of analytes.[66,67] Therefore, understanding analyte-induced disassembly of aptamer-linked AuNPs can help improve the general strategy for designing colorimetric sensors for many analytes.

## Materials and Methods

**Materials.** All DNA samples were purchased from Integrated DNA Technologies, Inc (Coralville, IA). The linker DNA was purified by polyacrylamide gel electrophoresis, while the thiol-modified DNA was purified by standard desalting. All nucleosides and cocaine were purchased from Aldrich (St. Louis, MO).

**AuNP Preparation and Functionalization.** AuNPs (40-nm diameter) were purchased from Ted Pella, Inc. (Redding, CA). AuNPs (13-nm diameter) were prepared by standard citrate reduction method described in the literature.[23,33] Thiol-modified DNA molecules were first activated by 1.5 equiv of TCEP for 1 h under pH 5.2 at room temperature before use. Glass vials (20-mL volume) were soaked in 12 M NaOH for 1 h and rinsed with DI water before use. AuNPs were loaded into the NaOH-treated glass vials, and thiol-modified DNA was added to a final concentration of 3 $\mu$M. The vials were capped and kept at room temperature for ~16 h. Tris acetate buffer (pH 8.2) was then added to the nanoparticles to a final concentration of 5 mM, and NaCl was added to a final concentration of 100 mM. The AuNPs were used within 3 days after functionalization.

**Preparation of AuNP Aggregates.** To assemble AuNPs, two kinds of AuNP of choice (200 $\mu$L each) were mixed and centrifuged at 13.2 krpm for 8 min. The supernatant was removed and replaced with a buffer containing 100 mM NaCl and 25 mM Tris acetate, pH 8.2. The sample was centrifuged again to remove the supernatant once more. Then the AuNPs were dispersed in 300 mM NaCl, 25 mM Tris acetate, pH 8.2. Appropriate linker DNA was added at a final concentration of 100 nM. After processing, the final absorption of AuNPs was ~2.2 at 522 nm. The samples were allowed to stay at 4 °C overnight. For head-to-tail aligned AuNPs, the aggregates were formed in 48 h. The aggregates were centrifuged briefly with a benchtop microcentrifuge and precipitated to the bottom of the microcentrifuge tube. The supernatant was removed, and new buffer was added (300 mM of NaCl and 25 mM of Tris acetate, pH 8.2). Such a solution can be used as a sensor for adenosine detection.

**Monitoring of Disassembly by UV−Vis Spectrometer.** In a UV−vis sampling cell, 48 $\mu$L of the buffer (25 mM Tris acetate, pH 8.2, no NaCl) was first added. Then 50 $\mu$L of the above-prepared AuNP aggregates was added, so that the final NaCl concentration was ~150 mM. The cell was allowed to sit in a temperature-controlled sample chamber for 5 min to reach the designated temperature. The spectrometer (Hewlett-Packard 8453) was set to collect spectra at 10-s intervals. After pushing the start button, adenosine (2 $\mu$L of 50 mM) was added immediately to the cell and the cell was placed back to the sample chamber to allow the spectrometer to acquire the rest of the spectra. For experiments that varied NaCl or pH, slightly modified protocols were employed.

**Melting Curves.** Melting curves were measured on the temperature-controlled UV−vis spectrometer by monitoring the extinction of samples at 260 nm. After reaching each designated temperature, the sample was allowed to sit in that temperature for another 2 min before we took a spectrum. The cuvette was covered by Parafilm to avoid evaporation. Samples with AuNP aggregates were agitated by shaking before taking each spectrum to prevent precipitation of aggregates. The melting curves were normalized in such a way that the initial $E_{260}$ was 0.6 and the final $E_{260}$ was 1.2.

**Aptamer Beacon Experiments.** Aptamer beacons were annealed with 100 nM fluorescein-labeled DNA, 200 nM aptamer linker, and 400 nM quencher-labeled DNA in 150 mM NaCl, 25 mM Tris acetate, pH 8.2 from 60 °C to 4 °C over 2 h. The annealed beacons were diluted 10-fold in the same buffer to monitor melting curves or kinetics in the presence or absence of 1 mM adenosine. The temperature to monitor the kinetics was 10 °C for both beacons. The fluorescence excitation was at 473 nm, and emission was collected at 520 nm. For melting curves, fluorescence at 520 nm was monitored with temperature increase.

**Acknowledgment.** This material is based upon work supported by the National Science Foundation through a Science and Technology Center of Advanced Materials for Purification of Water with Systems (WaterCAMPWS) (CTS-0120978) and a Nanoscale Science and Engineering Center (NSEC) (DMR-0117792) program, and by the U.S. Army Research Laboratory and the U.S. Army Research Office under Grant No. DAAD19-03-1-0227.

**Supporting Information Available:** Data on cocaine aptamer-linked AuNPs, DNA sequence for aptamer molecular beacon, and UV−vis spectra of AuNPs before and after melting. This material is available free of charge via the Internet at http://pubs.acs.org.

JA072075+

(66) Wilson, D. S.; Szostak, J. W. *Annu. Rev. Biochem.* **1999**, *68*, 611−647.
(67) Jayasena, S. D. *Clin. Chem.* **1999**, *45*, 1628−1650.